The Simulation and Control of Ammonia Unit of Shiraz Petrochemical Complex, Iran

Fereshte Tavakoli Dastjerd and Jafar Sadeghi*

*Department of Chemical Engineering, Faculty of engineering,
University of Sistan and Baluchestan, Zahedan, Iran*

Abstract

The aim of this paper is the steady-state and dynamic simulations of the ammonia unit of Shiraz petrochemical complex and system behavior study versus the feed flow rate change for producing a good quality product. The ammonia unit consists of the reformer units, shift converter units, carbon dioxide absorption unit, methanation unit, and ammonia synthesis unit. For this purpose, in the first step, the ammonia unit is simulated at a steady state using the Aspen Plus 2006.5 simulator. In the following stage, the required parameters are entered into the software for the dynamic simulation. The Aspen Plus was exported to Aspen dynamic. In this study, PI and PID controllers, as basic controllers, were automatically added and tuned by the Tyreus–Luyben tuning method. Finally, in order to ensure the accuracy of the proposed control structure, the feed flow rate increased by 5%. The results show that, first of all, the simulation accuracy at steady and dynamic states are optimal so that the mean errors are -0.01% and -0.02% for steady and dynamic states, respectively. The controlling structure can well control the 5% feed increase.

1. Introduction

Ammonia is among the most important and expensive petrochemical products which is widely produced in the world and has a major role in the production of other chemical products. In Shiraz petrochemical complex, ammonia is produced by ICI model and Haber-Bosch method by the reaction of hydrogen and nitrogen gases in the vicinity of the iron catalyst. The simulation of chemical processes has always caught the interest of researchers. The steady-state simulation is suitable as a starting point in the simulation, but the chemical industries must increase productivity and profitability with the changes of market conditions. For this purpose, the dynamic plant study is used [1]. To understand the dynamic behavior of the chemical process and design, the process control systems require a dynamic process simulator [2]. Aspen dynamic simulator is designed for the dynamic process simulation [1]. Therefore, the implementation of dynamic process simulation and process optimization are important. Some of the done researches are mentioned as follows.

---

* Corresponding Author.
Tel./Fax: +98-54-33484077
Email: sadeghi@eng.usb.ac.ir (J. Sadeghi)

Reddy and Husaln (1982) simulated the ammonia synthesis loop and investigated the effects of the H_2/N_2 ratio of the return gas, loop pressure, recycle gas flow rate, and the concentration of inert gases on the ammonia production rate. The simulation results showed that the most important parameter is the H_2/N_2 ratio and its optimum value is around 2.5 [3]. Pedernera et al. (1999) simulated the ammonia synthesis loop in a steady state and investigated the effect of the manipulated variables on the reactor stability [4]. Rahimpour and Kashkooli (2004) developed a mathematical model for the removal of carbon dioxide from the synthesized gas into amine-promoted hot potash solution and investigated the influences of the important parameters of the model, such as amine addition and operating pressure on the absorption performance. The results showed that adding piperazine to potash solution carbonate increases the CO_2 absorption rate [5]. In order to determine the optimal inlet temperatures of the catalyst beds of an ammonia synthesis reactor, Akpa and Raphael (2014) maximized the objective function of the fractional conversion of nitrogen on the four catalyst beds of the reactor subject to variation of the inlet temperature to each catalyst bed. The results showed 42.38% increase in fractional conversion and 56.48% increase in ammonia concentration at the end of the fourth catalyst bed [6].

The purpose of this study is to simulate the ammonia unit of Shiraz petrochemical complex at steady and dynamic states using Aspen Plus 2006.5 and Aspen Dynamic 2006.5. In the steady state simulation, the kinetic equations of ammonia unit reactors are investigated. Also, suitable electrolyte data package is selected for the reactive absorption and reactive stripping of carbon dioxide. In order to simulate the dynamic state, control structures of subset units of ammonia unit are then investigated. Finally, in order to ensure the accuracy of the proposed control structure, 5% increase in feed flow rate is investigated.

2. Case Study

Fig. 1 shows the block flow diagram of ammonia production process at Shiraz petrochemical complex as following:

In the first step, the water vapor and sweet gas enter the pre-reformer reactor. In the pre-reformer reactor, the heavier hydrocarbons than methane in the feed are converted into methane and carbon monoxide (Reaction 1-5 in Table 1). The exhaust gases enter the primary reformer reactor. To produce the required hydrogen for ammonia synthesis loop, the methane cracking is performed (Reactions 6 and 7 in Table 1). Also, shift reaction occurs under the reforming conditions (Reaction 8 in Table 1). This reaction is exothermic and has a small equilibrium constant in reforming temperature. The exhaust gases with air stream enter the secondary reformer reactor. The secondary reformer reactor is an autothermal reactor where the air injection has two effects. First, the combustion of some gases increases the temperature (Reactions 9 and 10 in Table 1) that creates the needed temperature to complete the reforming reaction. Secondly, the air injection provides the required nitrogen of the synthesis stage and adjusts the H_2/N_2 ratio. The exhaust gases enter the High-Temperature Shift (HTS) reactor after passing through several converters. Conversion reaction (Reaction 12 in Table 1) is performed at 370 °C and the carbon monoxide quantity in the exhaust gas reduced to 3.3 mole fraction. The exhaust gases must be cooled before entering the Low-Temperature Shift (LTS) reactor. Conversion reaction (Reaction 13 in Table 1) is performed at 220 °C and the carbon monoxide quantity in the exhaust gas reduced to 0.4 mole fraction (dry basis). The exhaust gases are sent to the carbon dioxide absorption and stripping unit to remove carbon dioxide. Carbon dioxide absorption is carried out by the Benfield solution. The equilibrium reaction is performed at the absorption and stripping towers (Reaction 14 in Table 1). In order to remove the residual carbon monoxide and carbon dioxide, the exhaust gases are sent to methanation reactor (Reactions 15 and 16 in Table 1). The exhaust synthesized gases enter the compression stage. According to the ammonia production in the certain temperature and pressure, the gas pressure increases to 231.28×10^5 Pa by passing through four compressor stages (three main stages and a loop iteration stage). The compressed gases are sent to the ammonia synthesis reactor and at every circulation, 15 molar percentage of the gas is converted to ammonia (Reaction 17 in Table 1). Ammonia synthesis reactor of the Shiraz petrochemical complex consists of three fixed catalytic beds so that the gas flows to axial and radial forms. The ammonia synthesis reaction is exo-

thermic; therefore, temperature control is important. For this purpose, the Quench stream injection is used that keeps the reaction away from the equilibrium and raises the fractional conversion of nitrogen. Since the synthesized gas contains a small amount of methane from reforming unit and argon gas from the air, the small amount of synthesized gas exits the ammonia synthesis loop as purge gas in order to reduce the concentration of inert gases in the unit continuously. The exhaust ammonia temperature from synthesis reactor is cooled by passing through six converters and reaches the dew point temperature and then decrease in flash tanks with the decrease in pressure. The liquid mixture reaches the bubble point and finally, the liquid ammonia is separated. Because of the presence of a small amount of ammonia in flash gases, in order to fully extract the ammonia, these gases are sent to the recovery system. The recovery system contains the ammonia absorption and stripping towers, flash tanks and a number of heat exchangers and pumps.
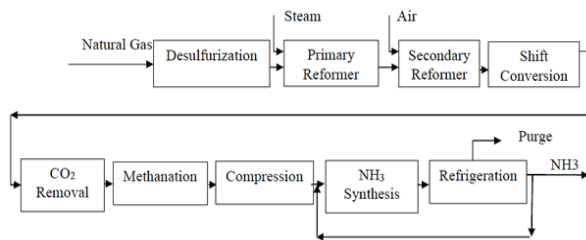

Figure 1. The block flow diagram of ammonia unit

3. Steady-state Simulation

The first step in the steady-state simulation of the process is the definition of the existing substances in the feed through the software database. The natural gas enters the ammonia unit at the pressure of 12.25 Pa. The second step is to choose the appropriate thermodynamic model. In ammonia unit simulation, two state equations are considered for different units. The carbon dioxide absorption unit has been converted into an aqueous electrolyte system because of the presence of the polar and electrolytic solvent of K_2CO_3 and the ELECNRTL state equation is used to calculate the activity coefficients of ions and molecules in solution. The Peng Robinson state equation was used in the reforming units, shift converters, methanation, and ammonia synthesis because of the presence of the non-electrolytic and polar materials,

non-polar materials and operation at pressures more than 10^6 Pa. The third step in the steady simulation was the installation of the appropriate flow currents and operating devices as follows.

3.1. Pre-reformer

In order to simulate the pre-reformer reactor, the stoichiometry reactor model was used because of the unavailability of the reaction kinetics.

3.2. Primary reformer

The primary reformer reactor contains 352 tubes with dimensions of 64 mm diameter and 12600 mm length. For simulating the primary reformer reactor from the Plug Model and the proposed kinetic equation, Froment [7] was used by the LHHW model presented in Table 2. The initial reformer catalyst specification is presented in Table 9.

3.3. Secondary reformer

The secondary reformer reactor has the dimensions of 3500 mm and length of 8500 mm. In addition to above three reactions, methane combustion is also carried out in this reactor. To define this reaction in the software, the Trimm and Lam [8] kinetic equation, which is presented in Table 3, was used. The characteristics of the secondary reformer catalyst are presented in Table 9.

3.4. Shift converters

The high and low-temperature shift reactors have the dimensions of 3400 mm diameter and 8500mm and 9300 mm lengths, respectively. The kinetic data of this reaction are different in two reactors, proportional to the temperature range, pressure, and type of catalyst. Rajesh [9] kinetic equation, presented in Table 4, was used in this regard. Table 9 presents the characteristics of catalysts for shift converters.

Table 1. The reactions of ammonia unit reactors

Equipment	Catalyst	Reaction	
Pre-reformer		$3C_2H_6 + H_2O \rightarrow 5CH_4 + CO$	(1)
		$3C_3H_8 + 2H_2O \rightarrow 7CH_4 + 2CO$	(2)
		$3C_4H_{10-1} + 3H_2O \rightarrow 9CH_4 + 3CO$	(3)
		$3C_4H_{10-2} + 3H_2O \rightarrow 9CH_4 + 3CO$	(4)
		$3C_5H_{12-1} + 4H_2O \rightarrow 11CH_4 + 4CO$	(5)
Primary reformer	Nickel	$CH_4 + H_2O \rightleftharpoons CO + 3H_2$	(6)
		$CH_4 + 2H_2O \rightleftharpoons CO_2 + 4H_2$	(7)
		$CO + H_2O \rightleftharpoons CO_2 + H_2$	(8)
Secondary reformer	Nickel oxide	(6),(7),(8)	(9)
		$2H_{2} + O_2 \rightarrow 2H_2O$	(10)
		$CO + O_2 \rightarrow CO_2$	(11)
		$CH_4 + 2O_2 \rightleftharpoons CO_2 + 2H_2O$	
HTS	Iron peroxide	$CO + H_2O \rightleftharpoons CO_2 + H_2$	(12)
LTS	Copper oxide , Zinc oxide	$CO + H_2O \rightleftharpoons CO_2 + H_2$	(13)
Carbon dioxide absorption system		$K_2CO_3 + H_2O + CO_2 \rightleftharpoons 2KHCO_3$	(14)
Methanation		$CO + 3H_2 \rightleftharpoons CH_4 + H_2O$	(15)
	Nickel	$CO_2 + 4H_2 \rightleftharpoons CH_4 + 2H_2O$	(16)
Synthesis reactor	Iron	$N_2 + 3H_2 \rightleftharpoons 2NH_3$	(17)

Table 2. The kinetic equations of reforming reactions

Reaction of reforming	kinetic equation	
$CH_4 + H_2O \rightleftharpoons CO + 3H_2$	$r_1 = k_1 \dfrac{\left(\dfrac{P_{CH4} \cdot P_{H2O}}{P_{H2}^{2.5}} - \dfrac{P_{CO} \cdot P_{H2}^{0.5}}{K_{eq1}} \right)}{DEN^2}$	
	$k_1 = 8.336 \times 10^7 \exp\left(\dfrac{-28879}{T} \right)$	$\left(\dfrac{mol. \ Pa^{0.5}}{kgcatalyst .s} \right)$
	$K_{eq1} = 10226.76 \times 10^6 \exp\left(\dfrac{-26830}{T} + 30.114 \right)$	(Pa^2)
$CH_4 + 2H_2O \rightleftharpoons CO_2 + 4H_2$	$r_2 = k_2 \dfrac{\left(\dfrac{P_{CH4} \cdot P_{H2O}^2}{P_{H2}^{3.5}} - \dfrac{P_{CO2} \cdot P_{H2}^{0.5}}{K_{eq2}} \right)}{DEN^2}$	
	$k_2 = 2.012 \times 10^{17} \exp\left(\dfrac{-29336}{T} \right)$	$\left(\dfrac{mol. \ Pa^{0.5}}{kg .s} \right)$
	$K_{eq2} = K_{eq1} \cdot K_{eq3}$	$\left(Pa^2 \right)$
$CO + H_2O \rightleftharpoons CO_2 + H_2$	$r_3 = k_3 \dfrac{\left(\dfrac{P_{CO} \cdot P_{H2O}}{P_{H2}} - \dfrac{P_{CO2}}{K_{eq3}} \right)}{DEN^2}$	
	$k_3 = 12.19 \exp\left(\dfrac{-8074.3}{T} \right)$	$\left(\dfrac{mol}{Pa .kg .s} \right)$
	$K_{eq3} = \exp\left(\dfrac{-4400}{T} - 4.063 \right)$	
	$DEN = 1 + K_{CO} P_{CO} + K_{H2} P_{H2} + K_{CH4} P_{CH4} + K_{H2O} \left(\dfrac{P_{H2O}}{P_{H2}} \right)$	
	$K_{CH4} = 6.65 \times 10^{-9} \exp\left(\dfrac{4604.28}{T} \right)$	(Pa^{-1})
	$K_{H2} = 6.12 \times 10^{-14} \exp\left(\dfrac{9971.13}{T} \right)$	(Pa^{-1})
	$K_{CO} = 8.23 \times 10^{-10} \exp\left(\dfrac{8497.71}{T} \right)$	(Pa^{-1})
	$K_{H2O} = 1.77 \times 10^5 \exp\left(\dfrac{-10666.35}{T} \right)$	(Pa^{-1})

Table 3. The kinetic equation of methane combustion reaction

Methane combustion reaction	kinetic equation
$CH_4 + 2O_2 \rightleftharpoons CO_2 + 2H_2O$	$T \geq 830\ (K)$ and $0.3 \leq \dfrac{O_2}{CH_4} \leq 5$ (molar ratio) $r_4 = \dfrac{k_a \cdot P_{CH4} \cdot P_{O2}}{(1 + K_{CH4}^{ox} \cdot P_{CH4} + K_{O2}^{ox} \cdot P_{O2})^2} + \dfrac{k_b \cdot P_{CH4} \cdot P_{O2}}{(1 + K_{CH4}^{ox} \cdot P_{CH4} + K_{O2}^{ox} \cdot P_{O2})}$ $k_a = 8.11 \times 10^{-8} \exp\left(\dfrac{-86}{RT}\right)$ $\left(\dfrac{kmol \cdot Pa^2}{kg\ catalyst \cdot s}\right)$ $k_b = 6.82 \times 10^{-8} \exp\left(\dfrac{-86}{RT}\right)$ $\left(\dfrac{kmol \cdot Pa^2}{kg\ catalyst \cdot s}\right)$ $K_{CH4}^{ox} = 1.26 \times 10^{-6} \exp\left(\dfrac{27.3}{RT}\right)$ (Pa^{-1}) $K_{O2}^{ox} = 7.87 \times 10^{-12} \exp\left(\dfrac{92.8}{RT}\right)$ (Pa^{-1})

Table 4. The kinetic equations of shift reactions

Shift reaction	kinetic equation	
$CO + H_2O \rightleftharpoons CO_2 + H_2$	$r_{co} = 0.0423\ \Psi\ k\left(y_{CO} \cdot y_{H2O} - \dfrac{y_{CO2} \cdot y_{H2}}{K}\right)$	$\left(\dfrac{kmol}{kg\ catalyst \cdot hr}\right)$
For HTS converter	$\Psi = 4$ $K = \exp\left(15.95 - \dfrac{4900}{T}\right)$ $K = \exp\left(-4.33 + \dfrac{4900}{T}\right)$	$\left(\dfrac{kmol}{kg\ catalyst \cdot hr}\right)$
For LTS converter	$\Psi = 4.33$ $K = \exp\left(12.88 - \dfrac{1855.5}{T}\right)$ $K = \exp\left(-4.33 + \dfrac{4577.778}{T}\right)$	$\left(\dfrac{kmol}{kg\ catalyst \cdot hr}\right)$

Table 5. The information of the reactive absorption and stripping towers

Tower	The type of packed components	HETP (m)	The height of the packed section (m)	The number of the equivalent equilibrium stages
Reactive absorption	103m³ 37mm Mini Ring S.S in 2 equal beds, 3100mm diameter, 216.4m³ 50mm Mini Ring S.S in 2 equal beds, 4500mm diameter	0.6	27.25	42
Reactive stripping	519m³ of 50mm Mini Ring S.S in 3 equal beds, 5500mm diameter	0.6	21.84	39

Table 6. The chemical reactions of the carbon dioxide absorption system

Carbon dioxide absorption system	Reactions
Absorption tower	$DEA^+ + H_2O \rightleftharpoons DEA + H_3O^+$
Stripping tower	$CO_2 + 2H_2O \rightleftharpoons H_3O^+ + HCO_3^-$
One valve	$HCO_3^- + H_2O \rightleftharpoons H_3O^+ + CO_3^{2-}$
One pump	$DEACOO^- + H_2O \rightleftharpoons DEA + HCO_3^-$
Two coolers	$2H_2O \rightleftharpoons H_3O^+ + OH^-$
	$K_2CO_3 \rightarrow 2K^+ + CO_3^{2-}$
	$KHCO_3 \rightarrow K^+ + HCO_3^-$

3.5. Carbon dioxide absorption unit

The carbon dioxide absorption system consists of two absorptions and stripping towers and a number of essential equipment in the fluid flow path between two towers. The carbon dioxide absorption and stripping towers were the packed column type. The performance of the packed towers was analyzed according HETP which is the ratio of the number of the equivalent equilibrium stages to the height of the packed section [10].

As shown in Table 5, the height of the filled section was calculated by the volume filled and the tower diameter.

The reactive absorption and reactive stripping towers contain the phase and chemical separation simultaneously. To simulate these towers, Rad Frac model, which is the exact model to simulate the chemical – phase equilibrium process, was used. Benfield solution, which contains potassium carbonate and Diethanolamine (DEA), is used for carbon dioxide absorption. To investigate the solubility of the carbon dioxide in the Benfield solution, ehotdebkp data package, which is the subset of the electrolyte data package, was used. This package considers the thermodynamic equilibrium between the phases and the kinetic effects of the reactions in aqueous solution, and also uses Henry's low constant to model the ionic strength of the inert gases, including hydrocarbons, hydrogen, nitrogen, etc. By enabling this package, the carbon dioxide absorption unit reactions, presented in Table 6, with their kinetic constants are defined in the Chemistry page from Reaction folder. The reactions are called chemistry which requires no catalyst.

3.6. Methanation

Methanation reactor has the dimensions of the 3400 mm diameter and 3400 mm length. The reverse reactions of the primary reforming are performed in the methanation reactor. Therefore, the kinetic data of reactions in the two reactors are similar to each other (Table 7). The catalytic characteristics of the methanation reactor are presented in Table 9.

3.7. Ammonia synthesis

To simulate the three catalytic beds of ammonia synthesis reactor, three plug model reactors were used. The first, second, and third beds have the dimensions of 2525 mm diameter and 2605 mm, 5210 mm and 7815 mm lengths, respectively. At first, in order to define this reaction, the modified equation of Temkin & Dyson [11], provided by LHHW model, was used. But this practical equation did not provide any suitable answer based on the process flow diagram information. Therefore, in order to get a suitable answer, the ammonia synthesis equilibrium reaction was defined to form the two separate reactions for software which is presented in Table 8. The kinetic data of two reactions was provided by POWER LOW model. The characteristics of the ammonia synthesis catalyst are presented in Table 9.

After completing the data on all devices and connecting all the flows except for a number of return flows, the simulation is completed (Figs. A1 and A2).

4. Dynamic Simulation

To convert the steady-state to dynamic simulation, the dimensions such as the height and diameter of reflux drum and sump and the hydraulic of trays of absorption and stripping towers were defined in a Dynamic page of equipment. Also the value of HETP was considered 0.6 meters. The dynamic simulation of ammonia unit was carried out based on flow driven and Implicit Euler integral method. To control each process, three steps were taken, including thermodynamic control, mass balance control, and quality control.

4.1. Thermodynamic control

The control of the appropriate and well-established thermodynamic conditions that was carried out using pressure control was related to the stability of the process.

One application of control systems is to increase the production capacity by increasing the feed flow rate. The feed increase leads to an increase in the input flow rate of the available compressors in the unit and reduces the output pressure of compressors. The output pressure changes of compressors influence the equipment performance such as flash vessels. To avoid problem creation, the output pressure of compressors was controlled by the power of the compressors. Also, the pressures of carbon dioxide absorption tower

and ammonia absorption and stripping towers were controlled by the vapor production rate of tower top and the heat duty of condenser used for controlling the pressure of carbon dioxide stripping tower.

4.2. Mass balance control

The mass balance control is related to the stability of the process. For mass balance control, the level control was used in the unit towers. Shiraz petrochemical ammonia unit consists of two carbon dioxide absorption and stripping towers and two ammonia absorption and stripping towers. In order to control the level of the towers, the sump level was controlled by the tower bottom product and the reflux drum level was controlled by the liquid product of tower top, but in the carbon dioxide stripping tower, the reflux drum level was controlled by the reflux flow rate because of the high reflux ratio.

4.3. Quality control

After controlling the process stability, quality control was carried out. In the following, the quality control of the products of the reactors and towers is investigated.

The kinetic constants of the reactions are the temperature function according to the Arrhenius'low [12]. Therefore, the temperature control is a proper choice for quality control, but on the other hand, the feed increase reduces the output temperature of the heaters and input temperature of the reactors. And this temperature change affects the reactor conversion rate. In order to prevent this problem, the input temperature of the reactors is controlled by the heat load of the heaters.

The ammonia synthesis reactor consists of three catalytic beds. To obtain the maximum product, the input flow of each bed must have the specified temperature. For this purpose, the input temperature to each bed was controlled by the input quench flow rate to the same bed. In towers, in order to raise the product quality, installing at least two quality controllers was essential. In the carbon dioxide stripping tower, to maintain the ratio of the vapor product flow rate of the tower to the feed tower, a multiplier was used. To control the temperature of the tray, the heat duty of

the reboiler was used. In this paper, a slope criterion was used to determine the appropriate temperature control tray. The temperature curve of the trays in the carbon dioxide stripping tower is presented in Fig. 2. As the figure shows, the drop in temperature occurs in trays No. 2 and 39. The trays No. 2 and 39 are the feed entry location and reboiler, respectively. The temperature between these two trays changes linearly and the tray No.36 of the carbon dioxide stripping tower was used to control the temperature by the heat duty of reboiler.
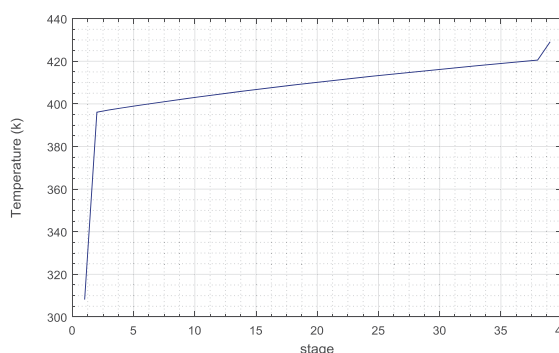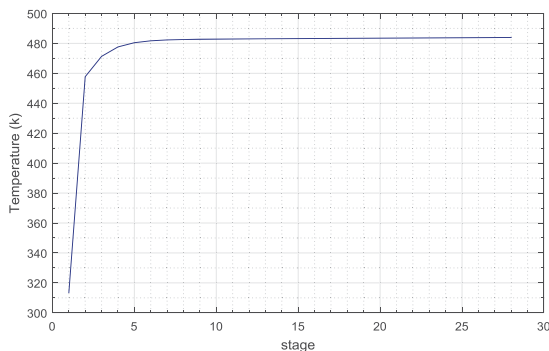

Figure 2. The temperature changes in carbon dioxide stripping tower trays

To control the ammonia stripping tower, the temperature of a tray at the top of the tower was controlled by reflux flow rate and the temperature of a tray at the bottom of the tower was controlled by heat duty of the reboiler. In order to select two appropriate trays to control the temperature, the temperature curve of trays was used. Fig. 3 shows the temperature changes of the trays. As the figure shows, the drop in temperature occurs in tray No. 2. The tray No.2 is the feed entry location. For this reason, it is not suitable for the temperature control. According to the slope criterion, the maximum temperature change occurs in the tray No. 3 and the temperature changes in the tower bottom trays are little. For this reason, in order to control the product quality, the temperatures of the trays No. 3 and 24 were controlled by the reflux flow rate and the heat duty of reboiler, respectively.

In the carbon dioxide absorption and stripping unit, a small amount of Diethanolamine absorbent is removed from the top of the absorption tower. In order to close the loop of this unit, the same

amount of Diethanolamine should be injected into the loop. Then the suitable controllers were located on the equipment of the ammonia synthesis unit and the return flow of this loop was closed. In the next step, the control unit for refrigeration and ammonia separation and the loop closure of absorption and stripping of ammonia were performed.

The main feed flow temperature, including the bulk of the reactor input feed, was less than the mixed return flow temperature with main feed flow. Thus, the reactor input flow had less temperature and followed by reducing the reactor output temperature. However, the output flow temperature became steady in less than an hour due to the existence of a temperature controller of the flow into the stoichiometric reactor.

Figure 3. The temperature changes in ammonia stripping tower trays

In the final step of the dynamic simulation of the process, the return flow should be closed from the ammonia feedstock preparation unit to the beginning of the process, but this loop will not close. This problem was solved by the change of the integration method. The Gear integration method is more suitable than the other integration methods. Therefore, the changes happen in solver options are presented in Table 10. Decreasing step size reduced the integral intervals and increased the precision of problem-solving. Thus, the dynamic simulation was completed (Figs. A3 and A4).

Figure 4. The pre-reformer reactor product changes

5. Results and Discussion

In this section, the results of increase in feed flow rate on the designed control structure accuracy is presented (Fig. A3 and A4). After reaching the simulated system to a steady state, the ammonia unit feed flow rate increased by 5% and the curves of several main streams were analyzed.

Fig. 4(a-c) shows the pre-reformer reactor product changes. The outlet flow rate from the reactor increased due to the increase in the input flow rate. Also, the temperature decreased at this time.

Figs. 5(a-c) and 6(a-c) show the Natural Gas Conversion Unit products. After increasing the feed intake, the discharge flow rate increased. Also, the output temperatures of two reactors decreased at this time because the input temperatures of two reactors declined and the endothermic reactions occured in these two reactors. But these temperatures were quickly controlled because the temperature controller was installed on the output flow of primary reformer. The output temperature of secondary reformer became steady after less than an hour.

Table 7. The kinetic equations of methanation reactions

Methanation reaction	kinetic equation
$CO + 3H_2 \rightleftharpoons CH_4 + H_2O$	$r_5 = k_1 \dfrac{\left(\dfrac{P_{CO} \cdot P_{H2}^{0.5}}{K_{eq1}} - \dfrac{P_{CH4} \cdot P_{H2O}}{P_{H2}^{2.5}} \right)}{DEN^2}$
$CO_2 + 4H_2 \rightleftharpoons CH_4 + 2H_2O$	$r_6 = k_2 \dfrac{\left(\dfrac{P_{CO2} \cdot P_{H2}^{0.5}}{Keq_2} - \dfrac{P_{CH4} \cdot P_{H2O}^2}{P_{H2}^{3.5}} \right)}{DEN^2}$

Table 8. The kinetic equation of ammonia synthesis reaction

Ammonia synthesis reaction	kinetic equation	
$N_2 + 3H_2 \rightarrow 2NH_3$	$r_7 = 10^{-6} \exp\left(\dfrac{-91000}{RT}\right) P_{H2}^3 \cdot P_{N2}$ $k = 10^{-6}$ $E = 91000$	$\left(\dfrac{kmol}{m^3 catalyst \cdot Pa \cdot s}\right)$ $\left(\dfrac{kJ}{kmol}\right)$
$N_2 + 3H_2 \rightarrow 2NH_3$	$r_8 = 13000 \exp\left(\dfrac{-142000}{RT}\right) P_{NH_3}^2$ $k = 13000$ $E = 142000$	$\left(\dfrac{kmol}{m^3 catalyst \cdot Pa \cdot s}\right)$ $\left(\dfrac{kJ}{kmol}\right)$

Table 9. The specifications of catalysts of the ammonia unit reactors

Equipment	Catalyst	Catalyst loading (kg)	Particle density (kg/cum)	Bed voidage
Primary reformer reactor	Nickel	1000	2000	-
Secondary reformer reactor	Nickel oxide	170	2500	-
High-temperature shift reactor	Iron peroxide	100	2500	-
Low-temperature shift reactor	Copper oxide, Zinc oxide	64	2500	-
Methanation reactor	Nickel	90000	-	0.9
Ammonia synthesis reactor	Iron	46000	-	0.9

Table 10. The solver option changes

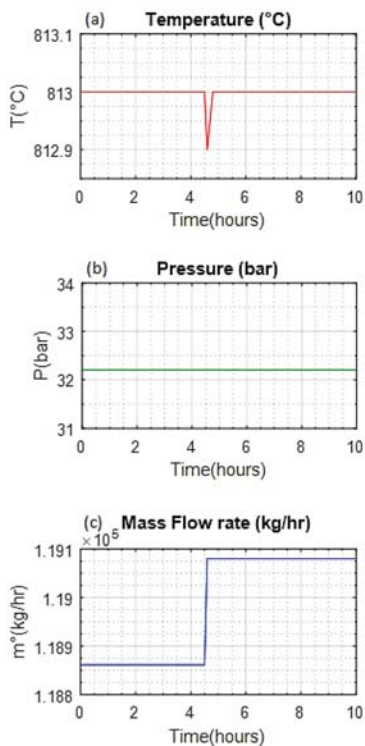| Solver options	Integration method	Initial step size	Minimum step size	Maximum step size
Initial	Implicit Euler	0.01	0.01	0.05
Final	Gear	1e-13	1e-13	0.001

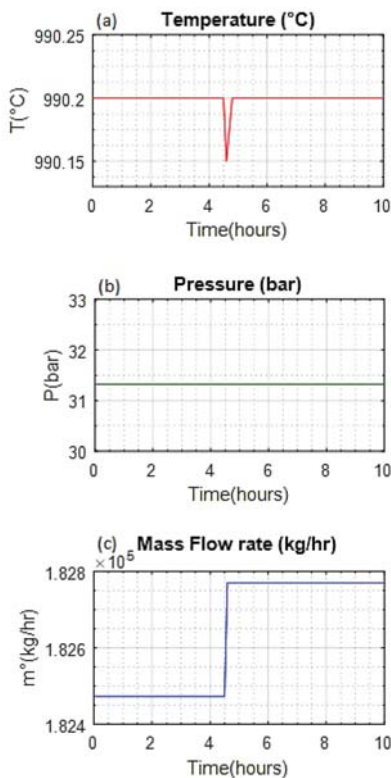**Figure 5.** The primary reformer reactor Product changes

Figure 6. The secondary reformer reactor product changes

Figs. 7(a-c) and 8(a-c) show the shift converter products. The flow rates from the reactors increased due to increased feed intake to the two reactors. Also, the output temperatures of two reactors increased at this time. The feed rise led to an increase in the reaction in these reactors and, on the other hand, the completed reactions in these two reactors are exothermic and this increased the output temperatures of the two reactors. However, the output temperatures of reactors became steady after less than an hour because the temperature controllers were installed on the input flows of shift converter reactors.
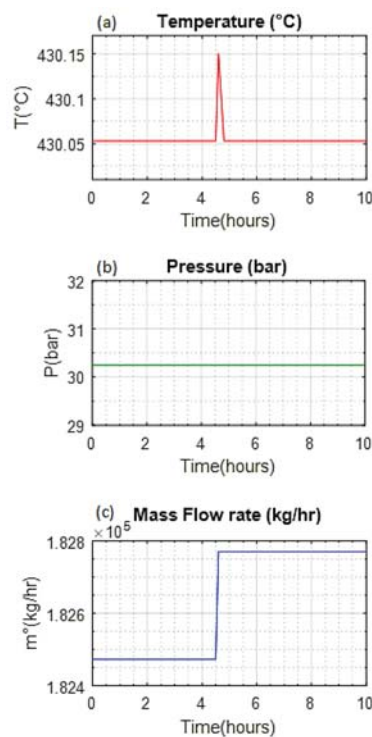
Figure 7. The high-temperature shift reactor product changes

Figs. 9(a-c) and 10(a-c) show the carbon dioxide absorption tower changes. The steam and liquid product rates of the tower increased due to increased feed intake to the tower at this time, the product temperatures of tower reduced. After making this disturbance, the feed temperature of the absorption tower decreased and the absorbent solution was not enough to absorb the carbon dioxide thereupon the amount of carbon dioxide absorption decreased. On the other hand, the absorption operation is exothermic and this led to the decrease in the temperature. However, the

output temperatures of absorption tower were steady after an hour because of the output carbon dioxide mole fraction control from the absorption tower top by the input water flow rate to loop and also the flow of the temperature control of input absorbent to absorption tower. The pressure curve changes revealed that the input feed increase increased the pressure in the tower and this increased the output pressures of this tower. However, the output pressures of the tower became steady after an hour because the inside pressure of the tower was controlled by the output vapor flow rate of the absorption tower.

duced the stripping operation and increased the output temperature of stripping tower, but the output temperatures of stripping tower became steady after an hour because the temperature of tray No.36 was controlled by the heat duty of reboiler. As you can see, the temperature changes in the products above the tower were higher than the bottom of the tower because the tray No. 36 is closer to the end of the tower and the temperature control in this tray reduced the effect of temperature turbulence in the lower tower products.

Figure 8. The low-temperature shift reactor product changes
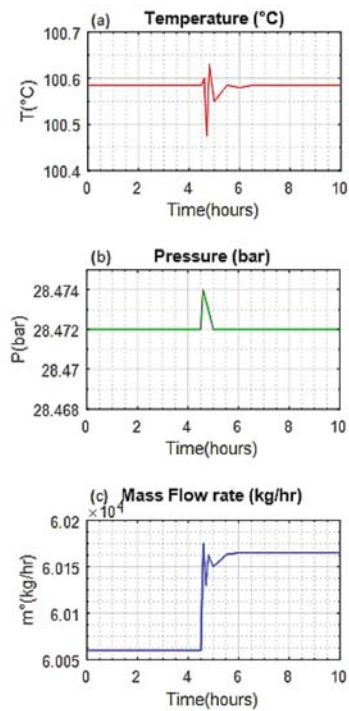
Figure 9. The carbon dioxide absorption tower vapor product changes

Figs. 11(a-c), 12(a-c) and 13(a-c) show the carbon dioxide stripping tower changes. The mass flow rates of stripping tower products increased and then reached a steady state due to the increase and fluctuations of the input feed. At this time, the temperatures of products above the tower increased. At first, the tower feed temperature was low and this affect the temperature profile in the tower and reduced the temperature in the tower. On the other hand, the stripping operation is endothermic. The temperature decrease re-

Fig. 14(a-c) shows the methanation reactor product changes. The mass flow rate of the methanation reactor product increased due to the increase and fluctuation of the input flow and then reached the steady state. At this time, the product temperature increased. The increase in feed increased the reactions in the reactor. On the other hand, the completed reactions in this reactor are exothermic and this increased the reactor product temperature, but because of fluctuations in the reactor feed, the output temperature of the reactor had the negligible fluctuations. With the stability of the feed flow rate and its temperature, the product temperature of methanation reactor became steady after l ess than two hours.
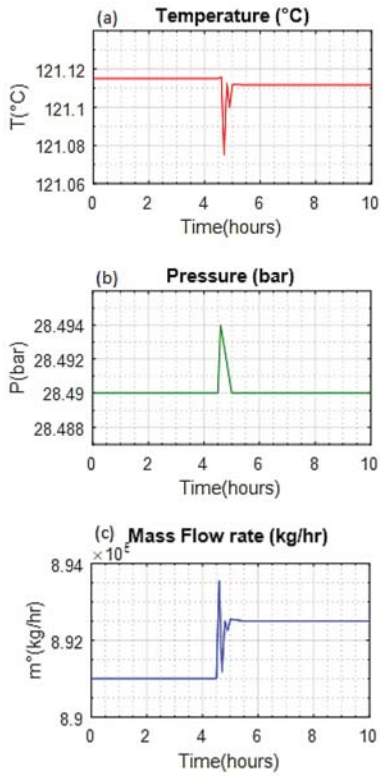
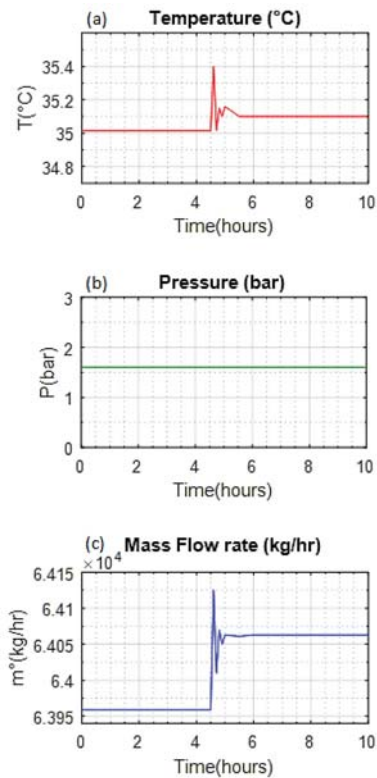**Figure 10.** The carbon dioxide absorption tower liquid product changes

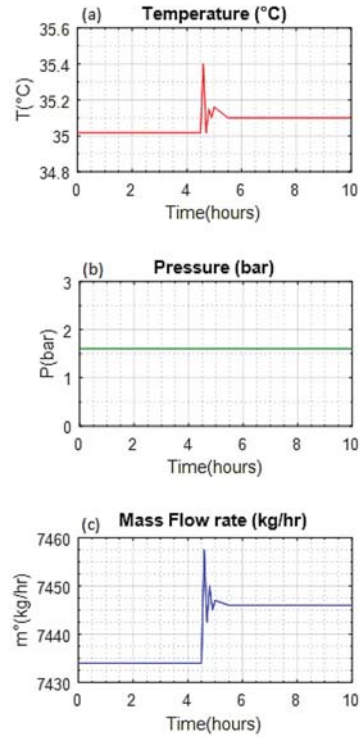**Figure 11.** The carbon dioxide stripping tower vapor product changes

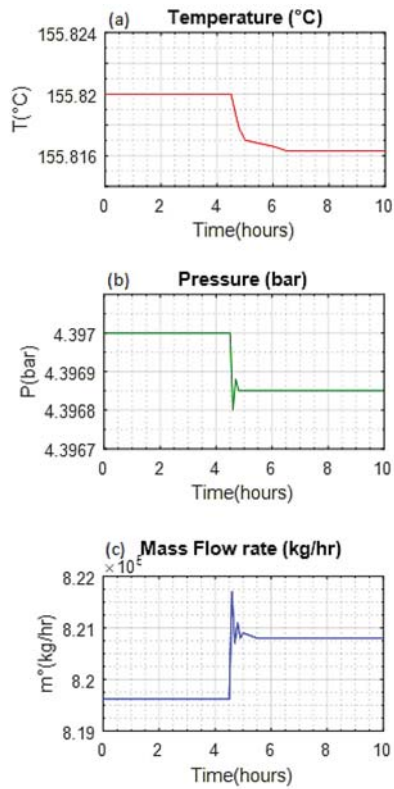**Figure 12.** The carbon dioxide stripping tower top liquid product changes

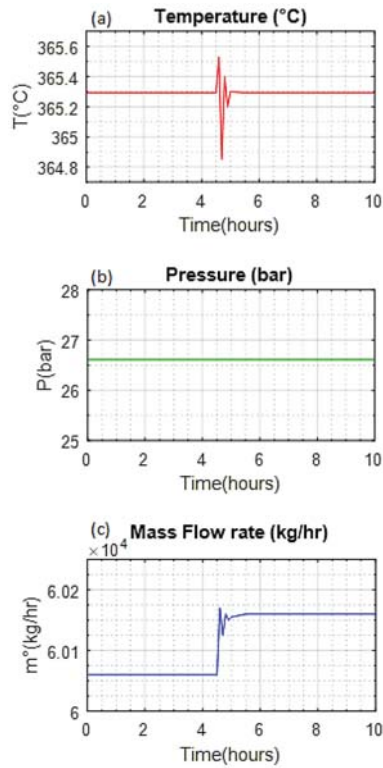**Figure 13.** The carbon dioxide stripping tower bottom product changes

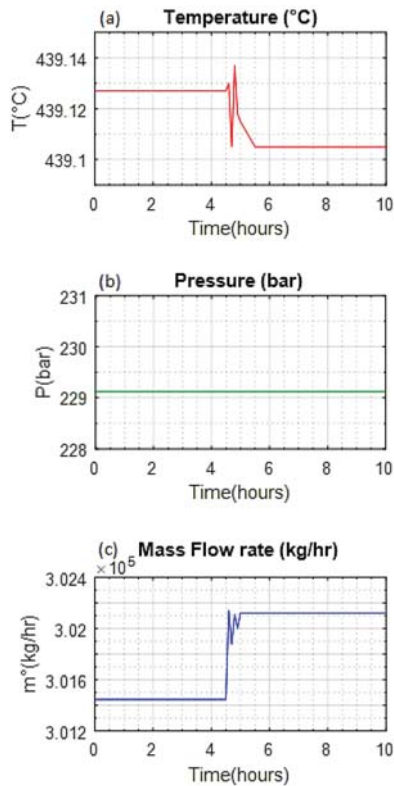**Figure 14.** The methanation reactor product changes

Fig. 15(a-c) shows the Ammonia synthesis reactor product changes. At the beginning of the change, the product temperature of the ammonia synthesis reactor decreased. The bulk of input feed to the third catalytic bed included the output flow from the second catalytic bed that its mass flow rate increased and as for the constancy of quench flow rate at the first, the input temperature of third catalytic bed increased. On the other hand, the ammonia synthesis reaction is exothermic and this temperature increase reduced the conversion rate in the reactor. As a result, the output temperature decreased. The output temperature was quickly controlled and this temperature became steady after one hour because the input temperature of third catalytic bed was controlled by the input quench flow rate to the same bed.

Fig. 16(a-c) shows the product changes. The product mass flow rate increased because of the feed flow rate increase. The temperature and pressure curves of the product have shown little changes. In the path of ammonia product refrigeration and separation, the extra temperature and pressure controllers were installed and followed by low disturbance effect. The product temperature became steady after one hour.
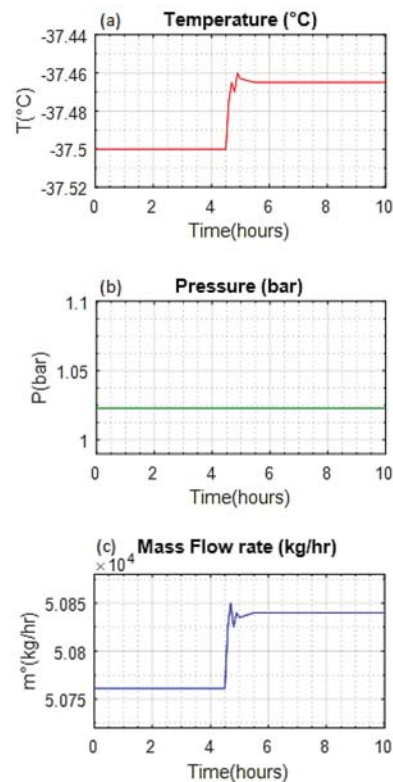

Figure 15. The ammonia synthesis reactor product changes

Figure 16. The product flow changes

6. Conclusions

In this article, the ammonia unit of the Shiraz petrochemical complex is simulated and analyzed in steady and dynamic states by the Aspen Plus 2006.5 and Aspen Dynamic 2006.5. 5% feed rate of the ammonia unit is also evaluated. The results are as follow:

- Certain units such as ammonia that is composed of several return flows and a lot of equipment, likely one or several return flows are not closed in a steady state.

- In order to investigate the carbon dioxide solubility in Benfield solution, ehotdebkp electrolyte data package is used that shows the ability of this electrolyte data package in the proper operation of the carbon dioxide absorption and stripping unit in the steady state.

- The applied electrolyte data package in carbon dioxide absorption and stripping unit result in the strong nonlinear behavior because of the numerous completed reactions in electrolyte space.

- The suitable thermodynamic equations for process simulation are ELECNRTL equation for carbon dioxide absorption and stripping unit and Peng Robinson equation for other subset units of the ammonia unit of the Shiraz petrochemical complex.

- In case of nonlinear units, such as ammonia unit, in order to eliminate the undesirable effects of strong nonlinear behavior sections of the unit to other sections, it is suitable to open the return flows and install the controllers of each section. Then the return flows are closed.

- The nonlinear behavior in the loop of carbon dioxide absorption and stripping unit shows that in addition to the installation of pressure, level and temperature controllers on the towers, the control of output carbon dioxide amount from absorption tower is necessary.

- The available reactors in the unit are gaseous and have fast dynamic features. That is why versus the applied disturbances become steady at the least possible time.

- 5% increase in unit feed flow rate is well controlled and this shows that the designed control system is suitable and has the ability of the feed capacity increase.

Nomenclature

Symbols

E	Activation energy
ΔH_i	Heat of adsorption
k_i	Reaction rate constant
K_{eq}	Equilibrium constant
K_i	Adsorption constant
LHHW	Langmuir Hinshelwood-Hougen-Watson
p_i	Partial pressure
r_i	Reaction rate
R	Gas constant
T	Temperature
y_i	Mole fraction

References

[1] Khodadoost, M. and Sadeghi, J. (2011). "Dynamic Simulation of Distillation Sequences in Dew Pointing Unit of South Pars Gas Refinery." *Journal of Chemical and Petroleum Engineering*, Vol. 45, No.2, pp. 109-116.

[2] Bequette, B. W. (1998). "Process Dynamics Modeling, Analysis and Simulation." Prentice Hall PTR, New Jersey.

[3] Reddy, K. V. and Husaln, A. (1982). " Modeling and Simulation of an ammonia synthesis loop." *Industrial & Engineering Chemistry Process Design and Development* Vol. 21, No. 3, pp. 359-367.

[4] Pedernera, M. N., Borio, D. O. and Schbib, N. S. (1999). "Steady state analysis and optimization of a radial-flow ammonia synthesis reactor." *Computers & Chemical Engineering*, Vol. 23, pp. 783-786.

[5] Rahimpour, M. R. and Kashkooli, A. Z. (2004). "Modeling and simulation of industrial carbon dioxide absorber using amine-promoted potash solution." *Iranian Journal of Science & Technology*, Transaction B, Vol. 28, No. B6. pp. 656-666.

[6] Akpa, J. G. and Raphael, N. (2014). "Optimization of an ammonia synthesis convertor." *world Journal of Engineering and Technology*, Vol. 2, No. 4, pp. 305-313.

[7] Abashar, M. E. E., Alhumaizi, K. I. and Adris A. M. (2003). "Investigation of methane-steam reforming in fluidized bed membrane reactors." *Institution of chemical engineers*, Vol. 81, No. 2, pp. 251-258.

[8] De smet, C. R. H., De croon, M. H. J. M., Berger, R. J., Marin, G. B. and Schouten, J. C. (2001). "Design of adiabatic fixed-bed reactors for the partial oxidation of methane to synthesized gas. Application to production of methanol and hydrogen-for-fuel-cells." *Chemical engineering science*, Vol. 56, No. 16, pp.4849-4861.

[9] Rajesh, J. K., Gupta, S. K., Rangaiah, G. P. and Ray, A. K. (2001). "Multi-objective Optimization of industrial hydrogen plants." *Chemical engineering science*, Vol. 56, No. 3, pp. 999-1010.

[10] Seader, J. D., Henley, E. J. and Ropert, D. K. (2010). *Separation process principles*. 3rd. Ed. Chapter 6, John Wiley & Sons, Inc., Hoboken.

[11] Nikacevic, N., Jovanovic, M. and Petkovska, M. (2011). "Enhanced ammonia synthesis in multifunctional reactor with *in situ* adsorption." *chemical engineering research and design*, Vol. 89, No. 4, pp. 398–404.

[12] Levenspiel, O. (1999). *Chemical reaction engineering*. 3rd. Ed. Chapter 2, John Wiley & Sons, Inc., Hoboken.

Appendix A
Nomenclature

| Symbols	
C	Compressor
Ca	Comparator
CC	Component control
D	Flash vessel
E	Heat Exchanger
H	Heater
LC	Level Control
M	Mixer
P	Pump
PC	Pressure Control
R_1	Pre-reformer reactor
R_2	Primary reformer reactor
R_3	Secondary reformer reactor
R_4	High-temperature shift reactor
R_5	Low-temperature shift reactor
R_6	Methanation reactor
R_7	First catalytic bed of ammonia synthesis reactor
R_8	Second catalytic bed of ammonia synthesis reactor
R_9	Third catalytic bed of ammonia synthesis reactor
S	Splitter
Su	Sum
T_1	Carbon dioxide stripping tower
T_2	Carbon dioxide absorption tower
T_3	Ammonia stripping tower
T_4	Ammonia absorption tower
TC	Temperature Control
V	Valve
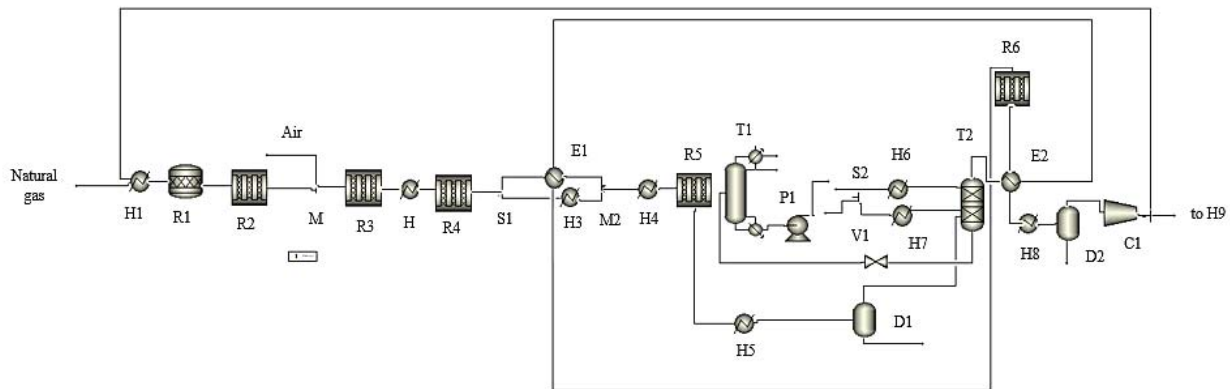
Figure A1. The process flow diagram of reforming, carbon dioxide absorption and methanation units in a steady simulation environment
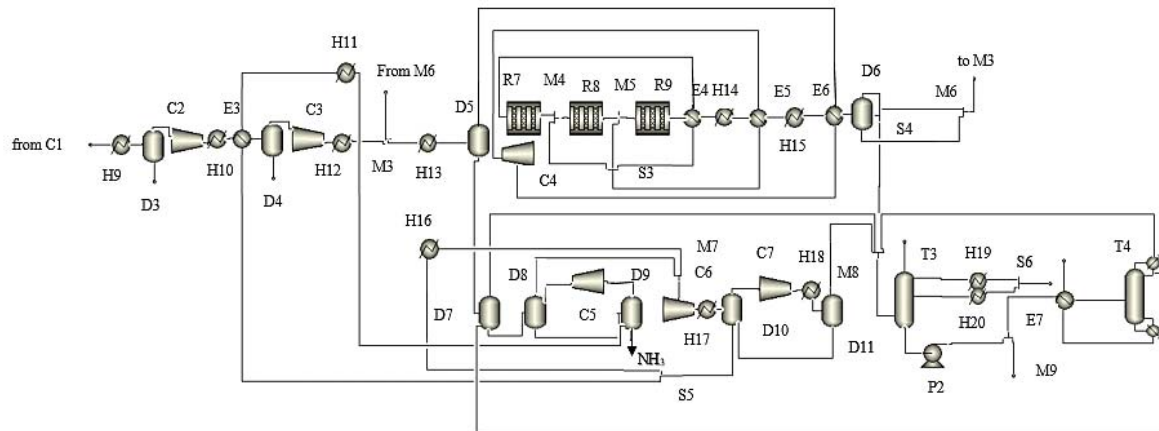
Figure A2. The process flow diagram of the ammonia synthesis, refrigeration and separation units in a steady simulation environment
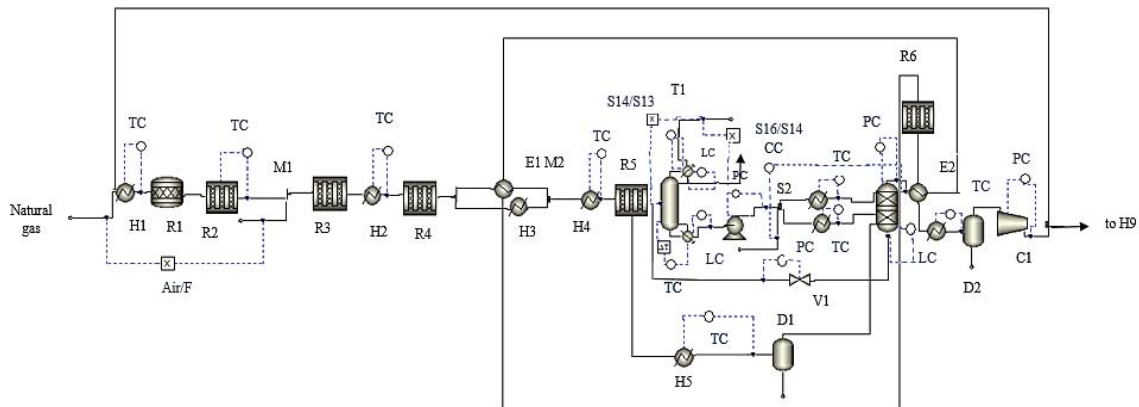
Figure A3. The process flow diagram of reforming, carbon dioxide absorption and methanation units in a dynamic simulation environment
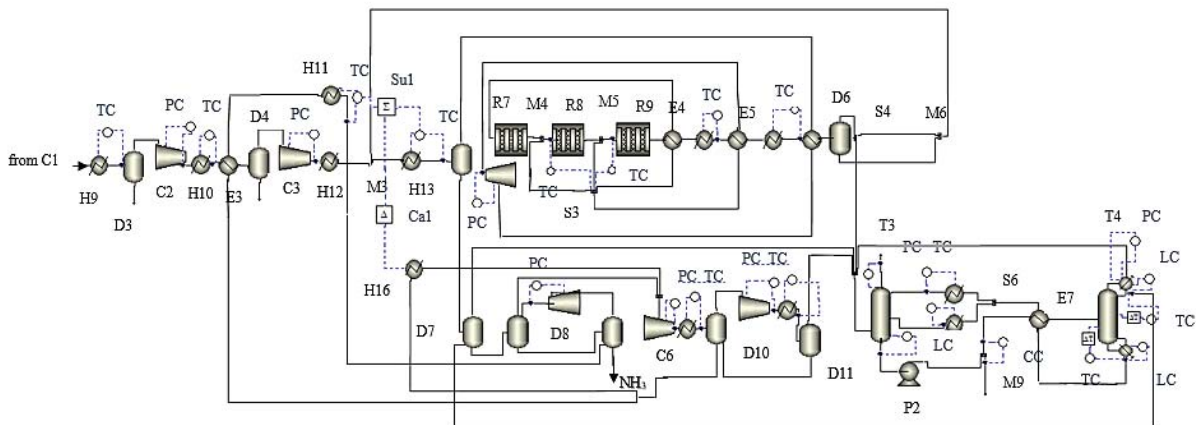
Figure A4. The process flow diagram of the ammonia synthesis, refrigeration and separation units in a dynamic simulation environment